Optica Applicata, Vol. XIV, No. 4, 1984

Equivalent grating configurations for concave holographic gratings

R. GÜTHER

Central Institute of Optics and Spectroscopy of the Academy of Sciences of GDR, 1199 Berlin–Adlershof, Rudower Chaussee 5, GDR.

We assume the vanishing of some coefficients of the aberration expansion of the light-path function for concave holographic gratings. Then two kinds of equivalent grating configurations can be defined. First, different production configurations which – for different wavelengths of use – yield the same correction behaviour as regards the selected aberrations (*configurations of the best correction*). Second, for a given configuration of production for every wavelength there exists a position of the illuminating slit, where the imaging quality is optimum in relation to the selected aberrations (*configurations of the best focussing*). Including *back-side production* of gratings we demonstrate some theorems which relate the configurations of best focussing to the configurations of best correction.

1. Introduction

Plane holographic gratings were first reported in paper [1]. Holographic concave gratings were discussed in papers [2, 3] and by other authors. In paper [4] we find the technique of back-side production for plane blazed holographic gratings. The back-side production of concave gratings is included in the systematic classification of stigmatic points in [5]. The production conditions of such concave gratings are widely discussed in papers [6] and [7].

In the following a production with two point sources in front of the grating is called the front-side production. A production is called a back-side one if one light source is situated in front of the grating, while a second convergent spherical light wave penetrates the grating support from the rear towards the front, a focussing point being in front of the grating. As in [5] we assume that the convergent back-side wave is a pure spherical wave. The aberrations resulting from the penetration of the grating support can be corrected by appropriate optical elements. The analytical treatment of such a correction is possible with a method outlined in [8].

In the framework of pure spherical waves for the production of front-side and back-side gratings we deal here with two questions. First, we suppose a grating with a given production configuration. For every wavelength of the spectral range we look for such positions of the slit that the images of the slit show vanishing low-order aberrations. The resulting curves for the slit

and its image are called *curves of the best focussing*. Second, a grating is given in a production configuration which is corrected in a special wavelength range. Then we look for a second grating of such a production configuration that another wavelength range is corrected, but positions of the slit and spectrum together with the image quality are the same as those of the first given grating. Since the second grating can do the work of the first grating in another wavelength range, this couple is called *equivalent gratings*. If the central wavelength within the wavelength range varies, the production configuration of the equivalent grating changes too. This means that the point sources used for production follow the curves which we call *equivalence curves* of the productions configuration.

Then there are relations between *the curves of the best focussing* and *the equivalence curves* in the back-side and front-side cases.

2. Equivalent production configurations and curves of the best focussing

We start with the lowest-order coefficients of the light-path function

$$F = \overline{AM} + \overline{BM} - \frac{k\lambda}{\lambda_0}(\overline{CM} + \overline{DM}) = \text{const} + GY + \tilde{D}Y^2 + \tilde{A}Z^2 + K1\,Y^3 + K2\,YZ^2 + \ldots \tag{1}$$

where A is the position of the slit, B – the image of the slit, C and D – the positions of the point sources used for production, G – the aberration coefficient yielding the grating equation, $\tilde{D}$ – the aberration connected with defocussing ($\tilde{D} = 0$ means meridional focussing), $\tilde{A}$ – the aberration responsible for astigmatism ($\tilde{A} = 0$ means sagittal focussing), $K1$ – the meridional coma and $K2$ – the astigmatic coma. In Figure 1 we show the usual configuration explaining the positions A, B, C and D in relation to the grating. We treat inplane gratings. For the description of A we use the angle α and the radial distance l_A. The expres-

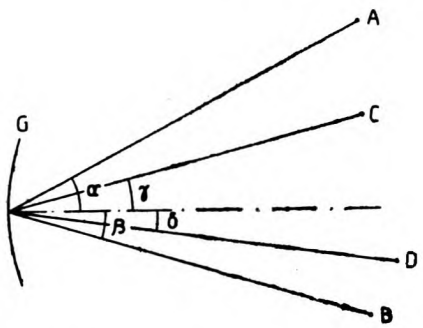

Fig. 1. Concave grating. Production by light sources C and D and use of the grating with a slit position A and its image B

sions for G, $\tilde{D}$, $\tilde{A}$, $K1$ and $K2$ can be taken from the well-known papers as, for example [2] or [3]:

$$G = -\sin\alpha - \sin\beta - \frac{k\lambda}{\lambda_0}(-\sin\gamma \mp \sin\delta), \tag{2}$$

$$\tilde{D} = \frac{\cos\alpha}{2}\left[\frac{\cos\alpha}{l_A} - \frac{1}{R}\right] + \frac{\cos\beta}{2}\left[\frac{\cos\beta}{l_B} - \frac{1}{R}\right] - \frac{k\lambda}{\lambda_0}\left\langle\frac{\cos\gamma}{2}\left[\frac{\cos\gamma}{l_c} - \frac{1}{R}\right] \pm \frac{\cos\delta}{2}\left[\frac{\cos\delta}{l_D} - \frac{1}{R}\right]\right\rangle, \tag{3}$$

$$\tilde{A} = \frac{1}{2}\left[\frac{1}{l_A} - \frac{\cos\alpha}{R}\right] + \frac{1}{2}\left[\frac{1}{l_B} - \frac{\cos\beta}{R}\right] - \frac{k\lambda}{\lambda_0}\left\langle\frac{1}{2}\left[\frac{1}{l_c} - \frac{\cos\gamma}{R}\right] \pm \frac{1}{2}\left[\frac{1}{l_D} - \frac{\cos\delta}{R}\right]\right\rangle, \tag{4}$$

$$K1 = \frac{\sin\alpha\cos\alpha}{2l_A}\left[\frac{\cos\alpha}{l_A} - \frac{1}{R}\right] + \frac{\sin\beta\cos\beta}{2l_B}\left[\frac{\cos\beta}{l_B} - \frac{1}{R}\right] - \frac{k\lambda}{\lambda_0}\left\langle\frac{\sin\gamma\cos\gamma}{2l_c}\left[\frac{\cos\gamma}{l_c} - \frac{1}{R}\right] \pm \frac{\sin\delta\cos\delta}{2l_D}\left[\frac{\cos\delta}{l_D} - \frac{1}{R}\right]\right\rangle, \tag{5}$$

$$K2 = \frac{\sin\alpha}{2l_A}\left[\frac{1}{l_A} - \frac{\cos\alpha}{R}\right] + \frac{\sin\beta}{2l_B}\left[\frac{1}{l_B} - \frac{\cos\beta}{R}\right] - \frac{k\lambda}{\lambda_0}\left\langle\frac{\sin\gamma}{2l_c}\left[\frac{1}{l_c} - \frac{\cos\gamma}{R}\right] \pm \frac{\sin\delta}{2l_D}\left[\frac{1}{l_D} - \frac{\cos\delta}{R}\right]\right\rangle. \tag{6}$$

The lower signs are related to the back-side production with pure spherical waves. Consequently, D (l_D, δ) designates the convergence point of the converging spherical wave.

Now, we treat *the curves of the best focussing*. For a given λ there is a position A of the slit which is *best* imaged on B. If we change λ then there are other positions A and B with *the best* imaging. Therefore A and B move along *the curves of the best focussing* when the parameter λ is changed.

What does *the best* imaging mean? We can demand that in (2) to (6) $G = \tilde{D} = \tilde{A} = K1 = K2 = 0$. Then we have the best imaging up to the third order. However, A and B are determined by the four parameters α, β, l_A, l_B, whereas there are five equations. We should demand that $G = \tilde{D} = 0$. Now, we can choose: $\tilde{A} = K1 = 0$ for the best anastigmatic imaging, or $K1 = K2 = 0$ ($\tilde{A} \neq 0$ mostly) for the astigmatic imaging with a small line width. There are cases in which the first possibility may be preferred (no astigmatism al-

lowed, for instance by the shape of a detector) and cases, where the astigmatism is not so critical as the line width (for example, in the usual monochromators).

Here we consider the first possibility, i.e., $G = \tilde{D} = \tilde{A} = K1 = 0$ or the system of equations:

$$\sin\alpha + \sin\beta = \frac{k\lambda}{\lambda_0}\{\sin\gamma \mp \sin\delta\}, \tag{7}$$

$$\cos\alpha\left[\frac{\cos\alpha}{l_A} - \frac{1}{R}\right] + \cos\beta\left[\frac{\cos\beta}{l_B} - \frac{1}{R}\right] = \frac{k\lambda}{\lambda_0}\left\{\cos\gamma\left[\frac{\cos\gamma}{l_c} - \frac{1}{R}\right] \mp \cos\delta\left[\frac{\cos\delta}{l_D} - \frac{1}{R}\right]\right\}, \tag{8}$$

$$\frac{1}{l_A} - \frac{\cos\alpha}{R} + \frac{1}{l_B} - \frac{\cos\beta}{R} = \frac{k\lambda}{\lambda_0}\left\{\frac{1}{l_c} - \frac{\cos\gamma}{R} \mp \frac{1}{l_D} \pm \frac{\cos\delta}{R}\right\}, \tag{9}$$

$$\frac{\sin\alpha\cos\alpha}{l_A}\left[\frac{\cos\alpha}{l_A} - \frac{1}{R}\right] + \frac{\sin\beta\cos\beta}{l_B}\left[\frac{\cos\beta}{l_B} - \frac{1}{R}\right] = \frac{k\lambda}{\lambda_0}\left\{\frac{\sin\gamma\cos\gamma}{l_C}\left[\frac{\cos\gamma}{l_C} - \frac{1}{R}\right] \mp \frac{\sin\delta\cos\delta}{l_D}\left[\frac{\cos\delta}{l_D} - \frac{1}{R}\right]\right\}. \tag{10}$$

The left side of this system of equations is given by λ_0 and by the production configuration parameters γ, δ, l_C and l_D. If we change λ, the nonlinear system of Eqs. (7) to (9) yields $\alpha(\lambda)$, $l_A(\lambda)$, $\beta(\lambda)$, $l_B(\lambda)$, these are *the curves of the best focussing.* Similar anastigmatic motions of this type are treated in [9, 10]. Schematically we formulate

$$\begin{bmatrix} \alpha \\ l_A \\ \beta \\ l_B \end{bmatrix} \begin{array}{l} \xleftarrow{\text{best focussing}} \\ \xrightarrow{\text{equivalent gratings}} \end{array} \begin{bmatrix} \gamma \\ l_C \\ \delta \\ l_D \end{bmatrix}. \tag{11}$$

The lower arrow means that imaging configuration $(\alpha, l_A, \beta, l_B)$ is given and we look for the solutions $\gamma(\lambda)$, $l_C(\lambda)$, $\delta(\lambda)$, $l_D(\lambda)$ of Eqs. (7) to (10) for different values of λ. Then, points C and D vary on *the equivalence curves.* If we produce a grating by two point sources on these curves, we obtain a grating corrected for the corresponding λ. This configuration is called K. Then we take another λ' and produce the configuration K' with C' and D' on *the equivalence curves.* Then the left sides of (7) to (10) do not change and any possible combinations of α, l_A, β, l_B yield for K and K' the same values of G, $\tilde{D}$, $\tilde{A}$ and $K1$. This means

that in both cases there are the same aberrations and, consequently, the same imaging behaviour up to $K1$.

For a, l_A, β, l_B being given the method of reduction of (7) to (10) down to a single equation of the unknown γ was demonstrated in [11].

Taking the function $\delta = \delta(\gamma)$ from (7) we calculate $l_C(\gamma)$ and $l_D(\gamma)$ from (8) and (9). After putting the expressions δ, l_C and l_D into Eq. (10) we obtain a single equation for γ which can be solved by Newton's elimination method.

If we take into account only the aberrations up to $K1$ we formulate:

Result 1. For every grating there are curves of the best focussing.

Result 2. For every grating there are equivalent production configurations which show the same properties in another wavelength range.

From this follows

Result 3. The curves of the best focussing show equal shape for the equivalent gratings.

Examples for Results 1 to 3 will be given in Chap. 4, after including the results of the next chapter.

3. Back-side production

The back-side production marked by the lower sign in (2)–(6) can also be formulated by the light-path function (1)

$$\Delta = \overline{AM} + \overline{BM} - \frac{k\lambda}{\lambda_0}(\overline{CM} + \overline{DM}) \tag{12}$$

where C is the source of the diverging spherical wave and D – the convergence point of the converging spherical wave. Equation (12) can be written in the form

$$\Delta = -\frac{k\lambda}{\lambda_0}\left(\overline{CM} + \overline{DM} - \frac{\lambda_0}{k\lambda}(\overline{AM} + \overline{BM})\right). \tag{13}$$

A constant factor in front of the light-path function has no consequences for the geometrical-optical imaging. Therefore, C and D in (13) can take the function of A and B, but then with the factor λ_0/k instead of $k\lambda/\lambda_0$. We obtain:

Result 4. We assume a set of equivalent gratings in relation to the configuration of use A and B. The curves of the best focussing for all these gratings are then identical with the equivalent curves of the grating production. The scale of wavelengths has to be changed.

The same argument can be used for the set of Eqs. (7) to (10), but the formulation with the full light-path function (13) is more general.

Another equivalence can be formulated by asking whether a back-side grating is equivalent to a front-side one. Then the four expressions in the

braces at the right side of Eqs. (7)–(10) for the front-side configuration (upper signs) γ_{front}, $l_{C\,\text{front}}$, δ_{front}, $l_{D\,\text{front}}$ should be equal to those with the back-side configuration (lower signs) γ_{back}, $l_{C\,\text{back}}$, δ_{back}, $l_{D\,\text{back}}$.

Assuming the front-side configuration we can calculate the equivalent back-side configuration and vice versa:

Result 5. Provided that there is the solution of the nonlinear system of equations, for a front-side grating there exists an equivalent back-side grating.

Since the production of configurations C and D of the set of equivalent back-side gratings is on the curves of the best focussing of these gratings we obtain:

Result 6. The curves of the best focussing for front-side gratings are identical with the *equivalent curves* of production configurations of the set of the equivalent back-side gratings.

4. Examples

We begin with a configuration of a grating: $\alpha = 41.424°$, $l_A = 20$ cm, $\beta = 7.424°$, $l_B = 20$ cm. We selected $\lambda_0 = 458$ nm and $R = 20$ cm as the additional parameters.

For both front-side and back-side productions we can use the elimination procedure described in Chap. 2 for obtaining the production configurations γ, l_C, δ, l_D by demanding $\tilde{A} = \tilde{D} = K1 = 0$ for any central correction wavelength $\lambda_{\text{centre of correction}}$. The configurations are shown in Table.

Equivalent front-side and back-side productions for a given configuration of use and for different centres of correction

$\lambda_{\text{centre of corr.}}$[nm]	Configuration for							
	Front-side production				Back-side production			
	γ[deg]	l_C[cm]	δ[deg]	l_D[cm]	γ[deg]	l_C[cm]	δ[deg]	l_D[cm]
300	60.696	18.506	−19.592	17.564				
400	46.751	19.183	−10.203	19.128				
500	40.320	19.829	−4.437	19.873	39.821	20.045	4.820	19.929
600	36.299	20.197	−0.669	20.266	36.304	20.218	0.665	19.724
700	33.513	20.424	1.988	20.498	33.333	20.383	−1.838	19.552
800	31.461	20.574	3.966	20.646	30.854	20.512	−3.445	19.424
1000	28.631	20.752	6.716	20.817	27.004	20.681	−5.270	19.266

In the back-side case the computer did not find an approximate solution for $\lambda_{\text{centre of correction}} = 300$ nm and 400 nm. We were also successful to find out back-side solutions for other α, l_A, β, l_B configurations in the range between 200 nm and 400 nm. The principles can be demonstrated by the values given in Table. All gratings in Table show the same astigmatism, defocussing and meridional coma. The values in this table demonstrate the Results 2 and 5.

We use these gratings as polychromators. This means that we fix the slit and look for meridional and sagittal focussing curves. Then we obtain Fig. 2. Each dot denotes a wavelength. If we choose the 500 nm grating, these points mark 19 equidistant wavelengths beginning with $\lambda = 350$ nm and ending with $\lambda = 800$ nm. From point to point there is a distance of 25 nm. The cor-

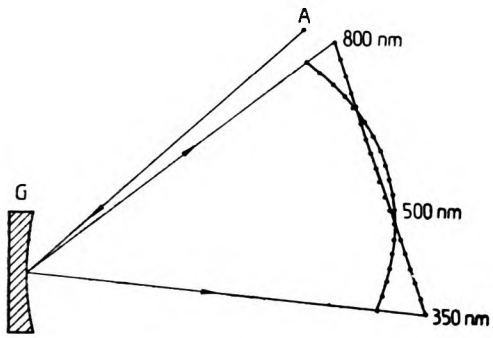

Fig. 2. The use of the equivalent gratings from Table as polychromators. The wavelengths apply to the 500-nm grating

rection point with 500 nm is the lower intersection of both curves. If the correction point corresponds to the wavelength of 400 nm, the wavelength interval begins with 280 nm and ends with 640 nm. Then the wavelength distance from point to point is 20 nm. In general, we assume two configurations with the correction wavelengths λ_1 and λ_2. The grating equations

$$\sin\alpha + \sin\beta = \frac{k\lambda_1}{\lambda_0}(\sin\gamma_1 + \sin\delta_1) = \frac{k\lambda_2}{\lambda_0}(\sin\gamma_2 + \sin\delta_2) \tag{14}$$

can be differentiated

$$d\beta\cos\beta = \frac{kd\lambda_1}{\lambda_0}(\sin\gamma_1 + \sin\delta_1) = \frac{kd\lambda_2}{\lambda_0}(\sin\gamma_2 + \sin\gamma_2) \tag{15}$$

From Eqs (14) and (15) we obtain by division

$$\frac{d\lambda_1}{\lambda_1} = \frac{d\lambda_2}{\lambda_2}. \tag{16}$$

This equation gives the result $d\lambda_2 = 20$ nm, for example $\lambda_1 = 500$ nm, $\lambda_2 = 400$ nm and $d\lambda_1 = 25$ nm.

If we use the gratings from Table in a monochromator mounting them with a pure rotation around the centre of the grating we obtain the meridional and sagittal focussing distances and the $K1$-values given in Fig. 3. The wavelength scale is valid for the 500 nm gratings. For other central wavelengths the λ-scale must be changed by Eq. (16).

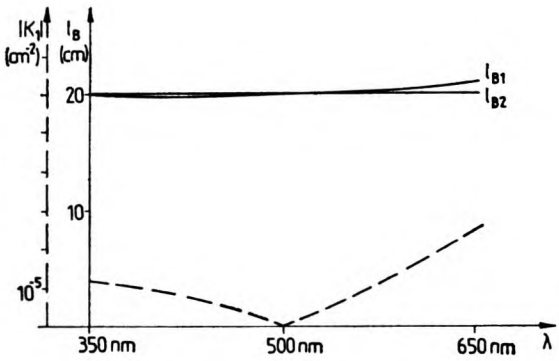

Fig. 3. The use of the equivalent gratings from Table as monochromators with a rotation mounting

The imaging quality is demonstrated by the ray tracings given in the Figs. 4–7. The aperture ratio is 1 : 3. In the monochromator case l_A and l_B are constant

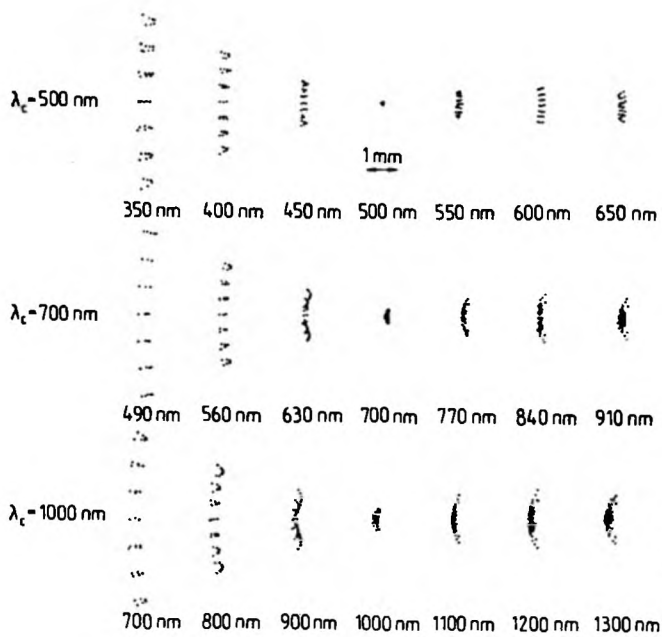

Fig. 4. Spot diagrams for the equivalent front-side gratings from Table used as polychromators

values. In the polychromator case we take the meridional focussing distance l_B for the distance between the plane of the spot diagram and the centre of the grating.

For the configurations given in Table we show:

— rays tracing for the set of front-side polychromators – in Fig. 4,
— rays tracing for the set of front-side monochromators – in Fig. 5,
— rays tracing for the set of back-side polychromators – in Fig. 6,
— rays tracing for the set of back-side monochromators – in Fig. 7.

The best correction occurs in a range near to the central wavelength. If the quality of correction decreases with the distance from the central wavelength, a new equivalent grating can be taken for a new central wavelength. The remaining aberrations show the form of the astigmatic coma, since this aberration has not been taken into account.

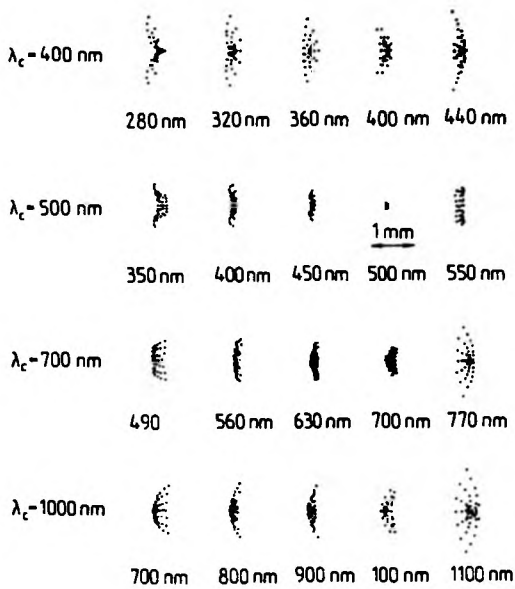

Fig. 5. Spot diagrams for the equivalent front-side gratings used as monochromators

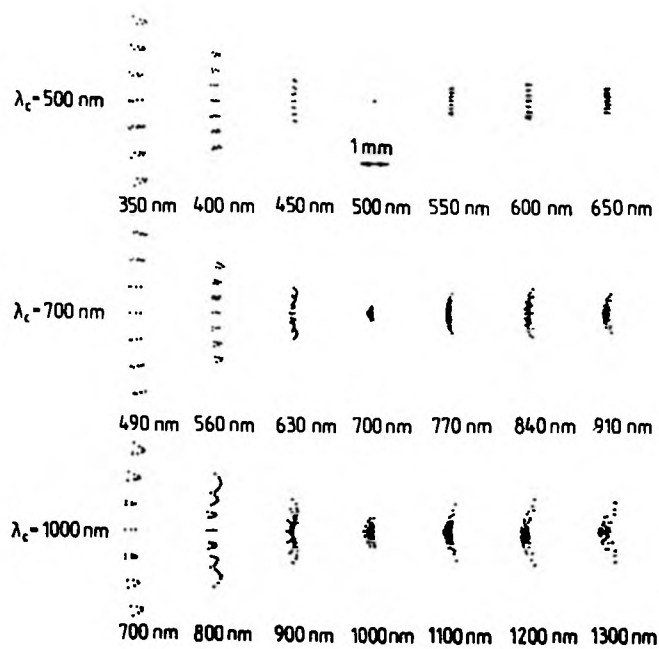

Fig. 6. Spot diagrams for the equivalent back-side gratings from Table used as polychromators

Now we show some examples connected with the curves of the best focussing. We begin with the back-side gratings from Table. The curves of equiv-

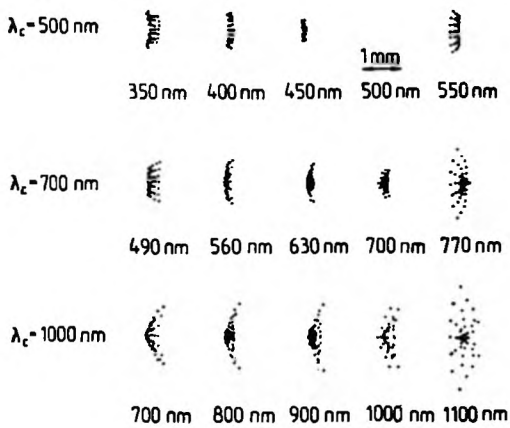

Fig. 7. Spot diagrams for the equivalent back-side gratings used as monochromators

alent production configurations for *C* and *D* are plotted in Fig. 8. Each point of the curves is marked by the wavelength of the centre of correction. We verify the Result 4 by writing in parentheses the wavelengths of the best

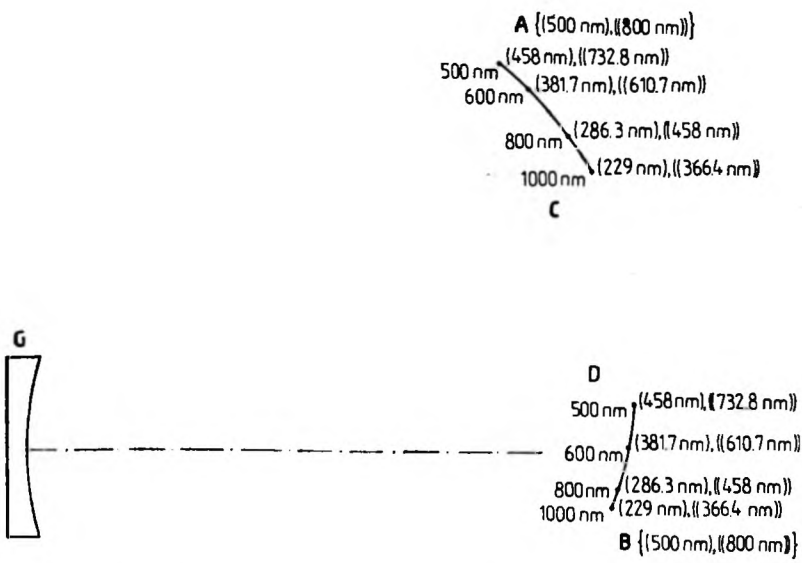

Fig. 8. Production configurations for the equivalent back-side gratings from Table (wavelengths without parentheses). These curves are also the ones of the best focussing for all front-side and back-side gratings (wavelengths in parentheses: 500-nm configurations, wavelengths in double parentheses: 800-nm configurations)

focussing if the curves to be the supports of A and B are interpreted, and if the underlying configuration is the 500 nm back-side grating from Table. The wavelengths in parentheses are calculated by

$$\lambda_{\text{best focus.}} = \frac{\lambda_0 500\ \text{nm}}{\lambda_{\text{centre of corr.}}}. \tag{17}$$

We can prove this formula by the following argument. The system of Eqs. (7)–(10) is written in a shortened form, for $k = 1$ and back-side production

$$\overline{AM} + \overline{BM} = \frac{\lambda}{\lambda_0}(\overline{CM} + \overline{DM}). \tag{18}$$

Equations (7)–(10) represent the first four expansion terms of (18) for the back-side case. Let λ_1 be the central correction wavelength of the investigated grating. In our example $\lambda_1 = 500$ nm. Then

$$\overline{A_1M} + \overline{B_1M} = \frac{\lambda_1}{\lambda_0}(\overline{C_1M} + \overline{D_1M}), \tag{19}$$

with (A_1, B_1) as the corresponding configuration of use with best focussing and (C_1, D_1) as a configuration of production. Then we look for the wavelength $\lambda_{\text{best focus.}}$ of a second configuration (A_2, B_2) on the curves of the best focussing of grating (C_1, D_1)

$$\overline{A_2M} + \overline{B_2M} = \frac{\lambda_{\text{best focus.}}}{\lambda_0}(\overline{C_1M} + \overline{D_1M}). \tag{20}$$

From Result 4 we know that, like (A_1, B_1) and (C_1, D_1), (A_2, B_2) is also located on the curves of the best focussing. Therefore, we find on these curves a production configuration (C_2, D_2) equivalent to (C_1, D_1), with $C_2 = A_2$ and $D_2 = B_2$. We look for $\lambda_{\text{best focus.}}$ of (A_2, B_2) expressed by the wavelength $\lambda_{\text{centre of corr.}}$ of (C_2, D_2). From Eqs. (19) and (20) and from the last remark, we obtain

$$(\overline{A_1M} + \overline{B_1M}) = \frac{\lambda_1}{\lambda_{\text{best focus.}}}(\overline{A_2M} + \overline{B_2M}) = \frac{\lambda_1 \lambda_0 / \lambda_{\text{best focus.}}}{\lambda_0}(\overline{C_2M} + \overline{D_2M}). \tag{21}$$

This means: (C_2, D_2) is equivalent to (C_1, D_1) as regards the wavelength $\lambda_{\text{centre of corr.}} = \lambda_1 \lambda_0 / \lambda_{\text{best focus.}}$. This results in Eq. (17).

Figure 8 is an example for Results 1, 2, 3, 4 and 6:

Result 1 – For the back-side grating the wavelengths in parentheses denote the positions of the best focussing (500-nm case).

Result 2. Equivalent grating production configurations are given by the wavelengths without parentheses.

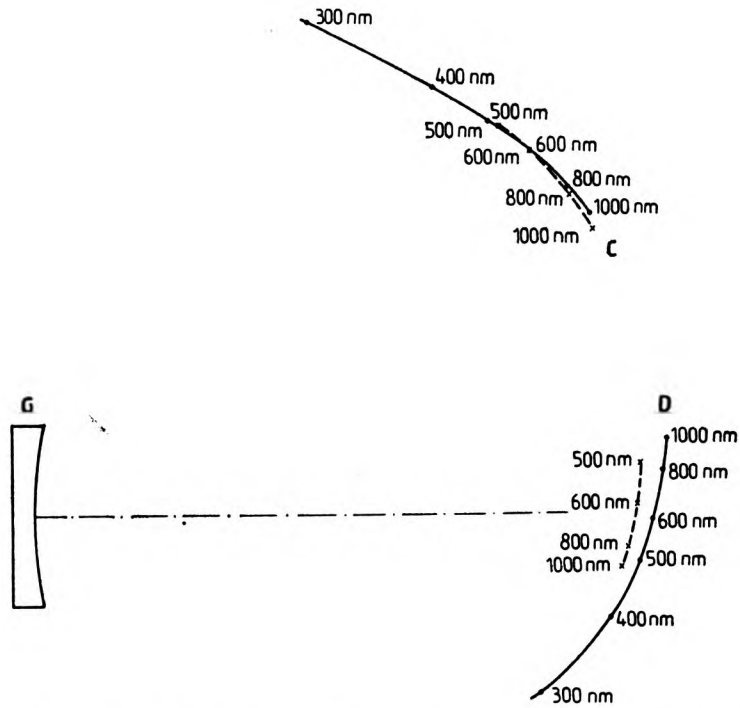

Fig. 9. Equivalent production configurations for back-side and front-side gratings from Table

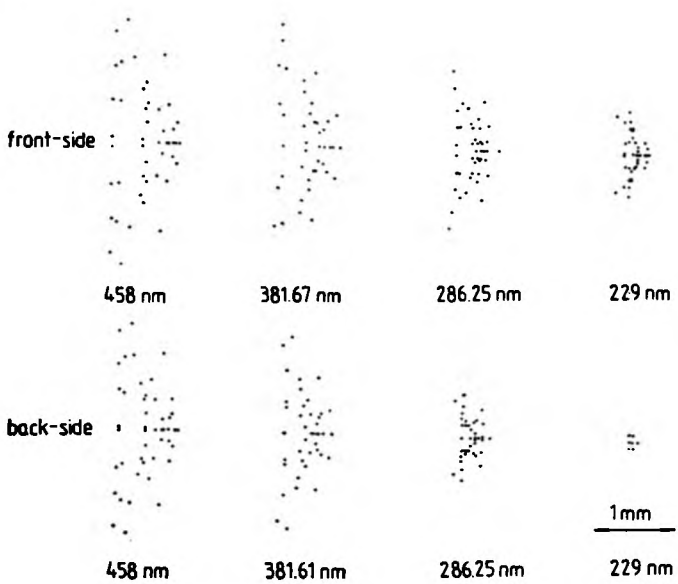

Fig. 10. Spot diagram of the curves of the best focussing for a front-side grating and an equivalent back-side grating

Result 3. The wavelengths of the curves of the best focussing are given in double parentheses for the back-side 800 nm case from Table.

Result 4. The curves of equivalent production configurations and the curves of the best focussing are the same for back-side gratings.

Result 6. The curves of the best focussing are identical for the set of front-side gratings and for the equivalent set of back-side gratings given in Table. The wavelengths in parentheses are related to both types.

We emphasize that for back-side and front-side gratings the curves of equivalent production configurations do not coincide. In Figure 9 we give a comparison of both kinds of curves. The positions C and D were taken from Table.

In Figure 10 we compare the spot diagrams of a ray-tracing procedure for a front-side grating and an equivalent back-side grating. The underlying gratings are the 500-nm gratings from Table. We see that the differences are small due to the neglected aberrations.

5. Discussion

The calculation of equivalent grating configurations is useful for finding gratings which work in different spectral ranges of the same properties. The methods developed above enlarge the well-known possibilities of wavelength change by using higher order diffraction [2].

The configurations of the best focussing show how to use a grating in an optimum way [12]. They are represented by a monochromator with complicated slit and exit slit motions. Their usage for testing was suggested [13].

We pointed out close relations between the curves of the best focussing and the equivalent curves of grating production.

Other definitions of equivalence are possible when generalizing the change of the spherical wavefront (given by the motion of A) by a change of the wavefront parameters in the second and higher orders [8].

References

[1] Rudolph D., Schmahl G., Umschau **67** (1967), 225.
[2] Hayat G. S., Flamant J., Lacroix M., Grillo A., Opt. Engin. **14** (1975), 420 (see also Jobin-Yvon, *Grating Handbook*).
[3] Namioka T., Seya M., Noda H., Jap. J. Appl. Phys. **15** (1976), 1181.
[4] Sheridon N. K., Appl. Phys. Lett. **12** (1968), 316.
[5] Palmer E. W., Hutley M. C., Franks A., Verrill J. F., Gale B., Rep. Prog. Phys. **38** (1975), 975.
[6] Obermayer H. A., Doctor's Thesis, Stuttgart, 1976.
[7] Hunter W. R., Appl. Opt. **21** (1982), 1634.
[8] Güther R., Optica Applicata **12** (1982), 451.
[9] Hisa M., Oshio T., Bull. Fac., Ed. Wakayama Univ., Nat. Sci. **30** (1981), 929; **31** (1982), 1.

[10] HISA M., OSHIO T., Opt. Acta **29** (1982), 1303.
[11] GÜTHER R., Optica Applicata **11** (1981), 413.
[12] GÜTHER R., Beiträge zur Optik und Quantenelektronik **7** (1982), 57 (*Frühjahrsschule Optik*, Leipzig 1982).
[13] FENSKE G., SCHUSTER R., KOHN H., Beiträge zur Optik und Quantenelektronik **7** (1982), 152 (*Frühjahrsschule Optik*, Leipzig 1982).

Received April 4, 1984

Эквивалентные конфигурации решеток для вогнутых голографических решеток

Предположено исчезновение некоторых коэффициентов разложения функции геометрических аберраций для вогнутых голографических решеток. Можно определить две эквивалентные конфигурации образуемых систем, которые для разной полезной длины волн дают тот же тип коррекции с точки зрения выбранных аберраций (конфигурации самых хороших поправок). С другой стороны, при данной образованной конфигурации существует одно положение трещины для каждой длины волны, для которого качество изображения оптимально по отношению к выбранной аберрации (конфигурация самого хорошего сжатия). Приведены некоторые теоремы, которые относят конфигурации самого хорошего сжатия к конфигурациям самых хороших поправок, также для случая *back-side production.*